

# Distributed Multinomial Regression

Matt Taddy

The University of Chicago Booth School of Business  
`faculty.chicagobooth.edu/matt.taddy`

This article introduces a model-based approach to distributed computing for high-dimensional-response multinomial logistic regression. Counts for each response category are treated as independent Poisson regressions via plug-in estimates for fixed effects shared across categories. We fit regularization paths for each regression and use information criteria to select coefficient estimates. The model provides a basis for distributed, rather than just parallel, statistical inference: such algorithms are essential in scaling to truly Big data that is too large to be stored or analyzed on a single machine, and we include a MapReduce recipe for application of the technique on distributed file systems. The work is driven by applications in multinomial inverse regression analysis of unstructured data, especially text, where large sets of documents are tokenized and the token counts are modeled as arising from a multinomial dependent upon document attributes. After some initial illustration in polychotomous regression, including consumer choice modeling for light beer purchases, the second half of the paper is a text mining case study in prediction and inference for reviews on the Yelp website.

# 1 Introduction

The likelihood for count data from a set of  $D$  independent Poisson trials factorizes as the product of a multinomial distribution for the individual counts conditional on the sum total across all trials and a Poisson distribution on this total. Say  $\mathbf{c}_i$  is a vector of counts in  $D$  categories, summing to  $m_i = \sum_j c_{ij}$ , and that each  $c_{ij}$  has been drawn independently  $\text{Po}(\lambda_{ij})$  – Poisson with intensity (i.e., mean)  $\lambda_{ij}$ . Then the multinomial is ‘embedded’ in the Poisson:

$$p(\mathbf{c}_i) = \prod_j \text{Po}(c_{ij}; \lambda_{ij}) = \text{MN}(\mathbf{c}_i; \boldsymbol{\lambda}_i/\Lambda_i, m_i) \text{Po}(m_i; \Lambda_i), \quad (1)$$

where  $\Lambda_i = \sum_j \lambda_{ij}$  and the multinomial denoted here has probabilities  $\lambda_{ij}/\Lambda_i$  and size  $m_i$ .

This well known connection has long been used by statisticians to justify ignoring whether sampling was conditional on margin totals in analysis of contingency tables. Birch (1963) showed that the maximum likelihood estimate (MLE) of  $\boldsymbol{\lambda}_i$  is unchanged under a variety of sampling models for 3-way tables *under the constraint* that  $\Lambda_i = m_i$ . This is satisfied at the MLE for a saturated model, with as many parameters as cells in the table. Palmgren (1981) extended the Birch work to log-linear regression models, with  $\lambda_{ij} = \exp[\alpha_j + \mu_i + \boldsymbol{\varphi}'_j \mathbf{v}_i]$ , where  $\mathbf{v}_i$  is a  $p$ -vector of covariates, for observations  $i = 1 \dots n$ . The Fisher information on  $\boldsymbol{\Phi} = [\varphi_1 \dots \varphi_d]'$  is the same regardless of whether or not you’ve conditioned on  $m_i$  (i.e., in either multinomial logistic regression or Poisson log regression) so long as  $\mu_i$  in the Poisson model is estimated at its conditional MLE,  $\hat{\mu}_i = \log\left(m_i / \sum_j e^{\alpha_j + \boldsymbol{\varphi}_j \mathbf{v}_i}\right)$ .

Traditionally, this connection is invoked when applying multinomial logistic regression: totals  $m_i$  are then ancillary and the  $\mu_i$  drop out of the likelihood. This paper takes the opposite view: if we are willing to fix estimates  $\hat{\mu}_i$  – potentially not at their MLE – then the factorized Poisson likelihood can be analyzed independently across response categories. Specifically, Section 2 argues for  $\hat{\mu}_i = \log m_i$  as a plug-in estimator that minimizes the bias from using Poisson likelihoods in place of a multinomial for log linear regression. We label this strategy, including penalized estimation and variable selection within each Poisson, distributed multinomial regression (DMR). It is available in the `distrom` package for R.

The idea is motivated by applications that involve very large response dimension  $D$ , as in multinomial analysis of text counts or other large categorical datasets (e.g. website visits

or consumer purchases). In particular, we'll apply the technique to the multinomial inverse regression (MNIR) of Taddy (2013c). In the original MNIR paper, the covariate dimension  $p$  was small and computation was made extremely fast by collapsing response counts across level combinations of these covariates. DMR extends MNIR to high-dimensional covariate sets where such collapsing is infeasible. Beyond MNIR, other authors working in web and text analysis who previously favored multinomial models – say, for latent factorization – are now using independent Poissons to scale for massive data; see Gopalan et al. (2013) as an example. From the perspective of this paper, such Poisson modeling strategies can be cast as Big data versions of their more common multinomial analogues.

These big- $D$  applications have the characteristic that  $m_i$  is random, and usually pretty big. For example, text mining  $m_i$  is the total word count in document  $i$ , and web analysis  $m_i$  would be the total count of sites visited by a browser. A Poisson model for  $m_i$  – the extra assumption made when moving from a multinomial to independent Poissons – is not far fetched, especially if  $\mathbf{v}_i$  includes a large number of covariates and fixed effects. However, we also find that DMR does very well for the more common polychotomous regression setting, where  $m_i = 1$  always. In our polychotomous examples, DMR with lasso penalization and under variety of selection rules performs at least as well in out-of-sample prediction as a cross validated lasso on the corresponding multinomial logistic regression model. DMR thus provides an every-day speedup in multinomial regression: even with small- $D$  response categories, you'll be able to fit the model almost  $D$  times faster in distribution (in simple shared-memory parallelization we observe speedups that are close to linear in  $D$ , depending upon machine architecture).

The body of this article starts in Section 2 with justification of our plug-in estimator  $\hat{\mu}_i = \log m_i$ . We then review in Section 3 penalized estimation and our use of the gamma lasso regularization path algorithm. This is followed in 4 with discussion of coefficient selection along these regularization paths. This can either occur on the basis of the independent Poisson likelihoods, or back on the grouped multinomial likelihood. We then break from methodology in Section 5 for two simple polychotomous regression examples – the small forensic glass data from R and a large panel of American light beer purchases.

The second part of the paper begins in Section 6 with an overview of the MNIR framework of Taddy (2013c). This includes an updated discussion of the opportunities opened if we al-

low for larger  $D$  than was considered in the original paper. Section 7 provides a MapReduce algorithm for distributed MNIR in analysis of Big unstructured datasets. Finally, we present in Sections 8 and 9 a two-part case study of publicly available Yelp online-review data. Section 8 considers prediction of review popularity (as scored by other Yelp users) from text and other attributes. Section 9 describes inference about the effect of user characteristics while conditioning on confounding information via text (and makes use of an additional scaling tool: the weighted least-squares approximation in Appendix A). We’ve found that inference problems of this type are a key application area for MNIR. Section 10 closes with a quick discussion.

## 2 Estimating baseline intensity

Consider multinomial logistic regression with linear equations  $\eta_{ij} = \alpha_j + \mathbf{v}'_i \boldsymbol{\varphi}_j$  for each observation  $i$  and response category  $j$ . The negative log likelihood is proportional to

$$\sum_{i=1}^n \left[ m_i \log \left( \sum_{j=1}^D e^{\eta_{ij}} \right) - \mathbf{c}'_i \boldsymbol{\eta}_i \right]. \quad (2)$$

It is easy to verify that adding observation fixed effects  $\mu_i$  to each  $\eta_{ij}$  in (2) leaves the likelihood unchanged. In contrast, the corresponding Poisson model, unconditional on  $m_i$ , has negative log likelihood proportional to

$$\sum_{j=1}^D \sum_{i=1}^n \left[ e^{\mu_i + \eta_{ij}} - c_{ij}(\mu_i + \eta_{ij}) \right] \quad (3)$$

with gradient on each  $\mu_i$  of  $g(\mu_i) = e^{\mu_i} \sum_j e^{\eta_{ij}} - m_i$ , and is clearly sensitive to these observation ‘baseline intensities’. As mentioned above, solution for the parameters of  $\eta_{ij}$  is unchanged between (2) and (3) if each  $\mu_i$  is set to its conditional MLE at  $\log m_i - \log \left[ \sum_j e^{\eta_{ij}} \right]$ .

Calculating conditional MLE for baseline intensities  $\mu_i$  requires communication across category dimensions ‘ $j$ ’. Since distributed computation precludes such communication, we’ll instead use  $\hat{\mu}_i = \log m_i$  as a simple plug-in estimator. Conceptually, we justify this choice being also the conditional Poisson MLE – the value that would lead Poisson estimates for  $\eta_{ij}$  to be unchanged from those based on the joint multinomial likelihood – in a few example models.

From (3), the gradient on  $\mu_i$  at this plug-in is  $g(\hat{\mu}_i) = m_i (\sum_i e^{\eta_{ij}} - 1)$ . Consider a saturated model where each  $\eta_{ij}$  is free. The Poisson MLE for  $\eta_{ij}$  will be  $\hat{\eta}_{ij} = \log(c_{ij}) - \hat{\mu}_i = \log(c_{ij}/m_i)$ , which gives  $g(\hat{\mu}_i) = 0$  and this value also minimizes the multinomial likelihood in (2). At the other extreme, consider an intercept-only model with  $\eta_{ij} = \alpha_j$ . The Poisson MLE is  $\hat{\alpha}_j = \log \sum_i c_{ij} - \log \sum_i e^{\hat{\mu}_i} = \log(\sum_i c_{ij}/M)$  where  $M = \sum_i m_i$ . The gradient is  $g(\hat{\mu}_i) = m_i(\sum_j \sum_i c_{ij}/M - 1) = 0$  so that we are again at the conditional MLE. Finally, consider a single binary covariate such that  $\eta_{ij} = \alpha_j + x_i \varphi_j$ ,  $x_i \in \{0, 1\}$ . Write  $C_{xj} = \sum_{i:x_i=x} c_{ij}$  and  $M_x = \sum_{i:x_i=x} m_i = \sum_j C_{xj}$ . Then the Poisson MLE are  $\hat{\alpha}_j = \log(C_{0j}/M_0)$  and  $\hat{\varphi}_j = \log(C_{1j}/M_1) - \log(C_{0j}/M_0)$ , so that we retain  $g(\hat{\mu}_i) = m_i \left( \sum_j C_{x_{ij}}/M_{x_i} - 1 \right) = 0$ .

These examples do not form a general result (things are more complicated with multiple correlated covariates, and especially under regularization), but they illustrate analytically why we might expect the performance we've seen empirically: estimates based upon  $\hat{\mu}_i = \log m_i$  do not suffer in out-of-sample validation. The resulting benefit is huge, as using a plug-in allows estimation of the Poisson regression equations to proceed in complete isolation from each other.

### 3 Gamma lasso regularization paths

Given baseline intensities fixed as  $\hat{\mu}_i = \log m_i$ , each of our  $D$  separate Poisson regressions has negative log likelihood proportional to

$$l(\alpha_j, \varphi_j) = \sum_{i=1}^n \left[ m_i e^{\alpha_j + \mathbf{v}'_i \varphi_j} - c_{ij}(\alpha_j + \mathbf{v}'_i \varphi_j) \right]. \quad (4)$$

This section will describe estimation via regularized minimization of these objectives. We drop the  $j$  response-category subscript for simplicity.

In high-dimensional analysis, likelihood maximization has been replaced by penalized likelihood maximization as the estimation tool-of-choice. Systems like (4) imply the penalized objective  $l(\alpha, \varphi) + n\lambda \sum_k c(\varphi_k)$ , where  $c$  is some positive cost function and  $\lambda > 0$  is a penalty weight. Such 'regularization' has a long history in engineering (e.g., from Tikhonov): you back away from optimality in exchange for robustness. A very common form in statistics is the lasso (Tibshirani, 1996), with  $c(\varphi_k) = |\varphi_k|$  an  $L_1$  cost function. The lasso (and other costs with a spike at zero) yield variable selection: some coefficient estimates will be set to exactly zero.

As the optimal value of  $\lambda$  is unknown and must be selected (see Section 4 below), efficient implementations of penalized estimation use path algorithms. In a ‘regularization path’, one starts at  $\lambda_1$  large enough such that the solution has  $\hat{\varphi}_j = 0$  for all  $j$ . The penalty weight is then incrementally decreased and coefficients are updated accordingly. Since the estimates corresponding to  $\lambda_t$  tend to be good starts for estimation at  $\lambda_{t+1}$ , such routines are extremely fast (and a path along, say, 100  $\lambda_t$  values can take less time than solving for the MLE once).

We will adopt the gamma lasso (GL) approach of Taddy (2013a). That article outlines a simple path algorithm for  $L_1$  penalization with variable-specific weights  $\lambda_t \omega_k^t$ . The GL is ‘adaptive’ in that the weights at segment  $t + 1$  depend on coefficient estimates from time  $t$  ( $\hat{\varphi}_k^t$ ) through the equation  $\omega_k^{t+1} = (1 + \gamma |\hat{\varphi}_k^t|)^{-1}$  where  $\gamma \geq 0$ . This includes the lasso if  $\gamma = 0$ . For  $\gamma > 0$  it provides fast ‘concave’ penalization, where the amount of extra cost applied to  $\hat{\varphi}$  is *decreasing* with the absolute value of this estimate. Concave penalization implies that strong signals (large  $|\hat{\varphi}|$ ) are estimated with nearly zero shrinkage. This is appealing in analysis of massive datasets, as it allows such signals to include the effect of any collinear variables and tends to yield sparser  $\hat{\varphi}$  (which is useful in reducing both storage and computation).

Even though GL paths have this nice feature of diminishing bias, each segment on the path requires only a simple  $L_1$  minimization. These are solved via coordinate descent within iteratively re-weighted least squares (IRLS), the algorithm in Taddy (2013a, Section 6), where each iteration has weights  $v_i = \lambda_i$  and ‘response’  $z_i = \log \lambda_i + y_i / \lambda_i - 1$ . Here,  $\lambda_i = m_i e^{\hat{\eta}_i}$  is the fitted intensity at current estimates (recall we’re suppressing the  $j$  subscript). A full overview of GL estimation is in the original paper, along with a general review of concave penalization. A central theme of the article is that one needs to understand the properties of the entire path in order to pick a single point estimate,  $\varphi^t$ . The following section tackles this issue for DMR.

## 4 Selection via Information Criteria

Penalized path estimation is a tool for enumerating a set of candidate models: all those along the grid  $\lambda_1 \dots \lambda_T$ . Think of the weights  $\lambda_t$  as a sort of *scquelch* that determines what you measure as signal and what you discard as noise. The framework is incomplete without a way to choose amongst possible  $\lambda_t$  values. This is a problem of model selection, and we will address the issue

through use of information criteria (IC; e.g., Efron, 2004).

We choose amongst candidate parameter estimates  $\{\hat{\Theta}_1 \dots \hat{\Theta}_1\}$  to minimize

$$\text{IC}(k) = 2l(\hat{\Theta}_t) + k \times df \quad (5)$$

where  $2l$  is fitted deviance,  $k$  is a complexity penalty and  $df$  is the number of degrees of freedom in minimization of  $l$ , the negative log likelihood. For the standard lasso,  $df$  is simply the number of nonzero parameters (Zou et al., 2007), while Taddy (2013a) provides a heuristic for calculating  $df$  under different levels of concavity in the gamma lasso.

There are two possible ways that IC can be applied in DMR. The first, perhaps more obvious, option has  $\Theta$  the full set of multinomial parameters,  $[\alpha, \Phi]$ , and  $2l$  is multinomial deviance. This scheme leads to a number of computational bottlenecks: since  $\lambda_t$  selection is shared across response categories, each Poisson regression regularization path needs to run on the same grid of penalty weights. Moreover, the full coefficient paths need to be passed back to a central machine for evaluation of multinomial deviance at each path segment (which can itself be expensive, due to the normalization required in calculating a multinomial likelihood).

As an alternative, we advocate independent *ungrouped* IC selection for each individual Poisson regression: there are  $D$  unique  $\Theta = [\alpha_j, \varphi_j]$  and  $l$  is the corresponding Poisson deviance. We do not include  $\hat{\mu}_i = \log m_i$  in the degrees of freedom accounting, such that  $df_j$  based on only  $[\alpha_j, \varphi_j]$ . In this set-up each Poisson regression has its own regularization path and selected coefficients correspond to a unique penalty weight  $\lambda_j^t$ . This speeds up computation by allowing calculation of initial  $\lambda_j^1$  to occur in parallel, by limiting communication to only the coefficient estimates at selected  $\lambda_j^t$  (instead of the entire paths), and by eliminating the need for any full multinomial likelihood evaluation. Moreover we find – despite what we may have hypothesized about the benefits of grouped selection – that the independent Poisson model IC selection performs at least as well as grouped multinomial selection in OOS validation.

The two most common IC rules are the AIC, with  $k = 2$ , and BIC, with  $k = \log(n)$ . Our experience is that with large  $n$  the BIC selects overly simple models, while for more covariates than observations the AIC overfits. The two options act as informal bounds on model complexity. In the examples here (which always have larger  $n$  than number of covariates), the

AIC is the best performer by a large margin in both grouped and independent selection.

Note that IC model selection is somewhat nonstandard – cross validation (CV), the procedure of looping over out-of-sample (OOS) prediction on left-out folds (subsets) of your data, is probably more common. We focus on IC here, and use CV only for validation of our various IC techniques, because the intent of the work is to offer massive scalability. Monte Carlo routines require significant extra time and communication overhead (plus thread-safe random number generation). However, there is nothing inherently wrong with CV selection in DMR; we hypothesize that CV rules applied to each independent Poisson regression will do very well.

## 5 Polychotomous regression examples

Before moving to big- $D$ , MNIR, and our Yelp case study, we look at the (surprisingly strong) performance of DMR in simple  $m_i = 1$  polychotomous regression.

### 5.1 Glass shards

Our first illustration uses the small ‘forensic glass’ dataset from Venables and Ripley (2002), available in the MASS library for R under the name `fgl`. The data are 214 observations on fragments of glass collected in forensic work. The response of interest is glass type: window float glass (`WinF`), window non-float glass (`WinNF`), vehicle window glass (`Veh`), containers (`Con`), tableware (`Tabl`) and vehicle headlamps (`Head`). Covariates for each shard are their refractive index and %-by-weight composition amongst 8 oxides.

The response here is a single category, such that  $m_i = 1$  and  $\hat{\mu}_i = 0$  for all  $i$ . This clearly violates the assumption of Poisson generation:  $m_i = 1$  is not random. However, `dmr` still works: multinomial models obtained from the fitted Poisson model regularization paths, either using IC or CV selection, perform as well as CV selected models from a lasso path for multinomial logistic regression (as implemented in the `glmnet` package for R). Maximum OOS  $R^2$ , calculated for multinomial deviance, is about 33% for both.

Poisson lasso (GL with  $\gamma = 0$ ) regularization paths for each glass type are shown in Figure 1, with the selected coefficients marked for AIC and BIC applied independently to each Poisson model. Out-of-sample performance is illustrated in the left panel of Figure 2, and can be

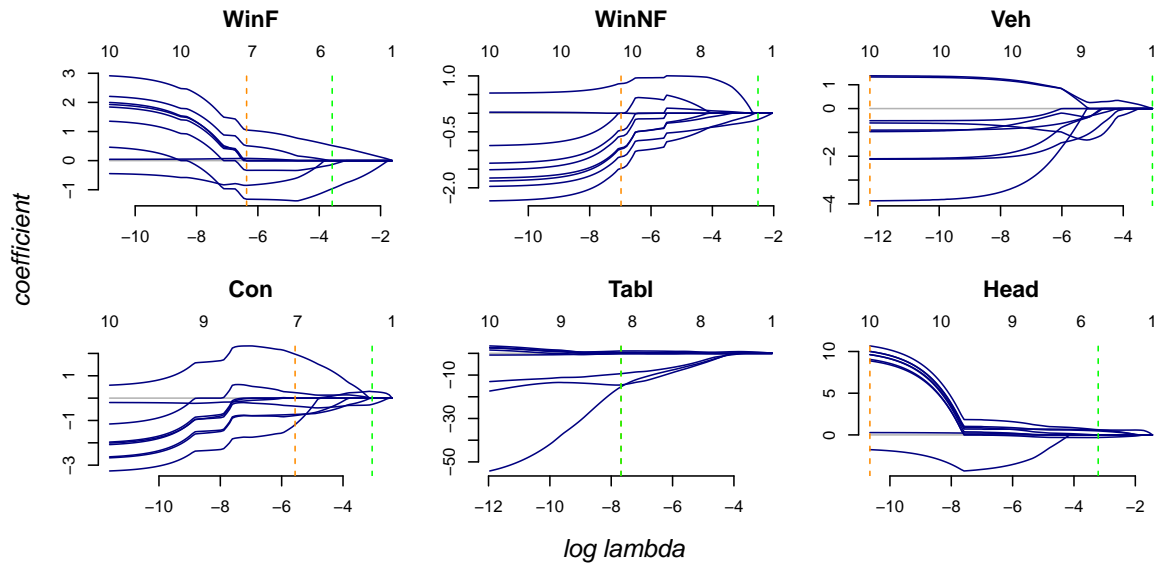


Figure 1: *Forensic Glass*. Regularization paths for each glass-type response category. AIC and BIC selections are marked with dashed vertical lines (orange and green respectively; they overlap for `Tabl`).

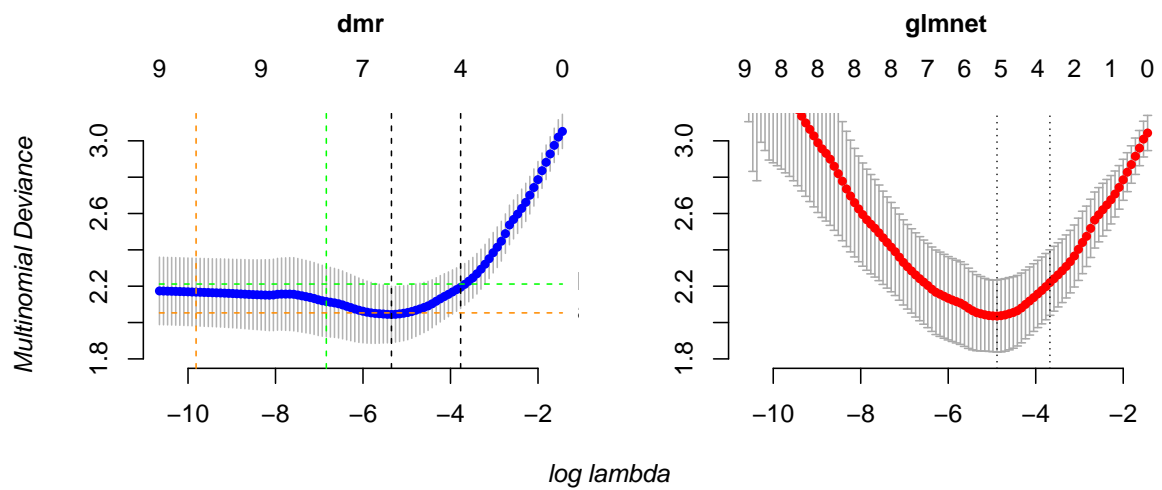


Figure 2: *Forensic Glass*. OOS deviance for `dmr` and `glmnet` in 20 fold CV. Dots are mean and segments show  $\pm 1$ se. The vertical dashed lines mark CV and IC shared  $\lambda_t$  selections, with black for CV (min and 1se), green BIC and orange AIC. Horizontal lines are mean OOS deviance for response-specific IC selections. The top axis is the mean number of nonzero coefficients across response categories.

compared against that of `glmnet` in the right panel. Here, and throughout this paper, we use the same 20 folds for both DMR and `glmnet` experiments. The vertical lines mark shared  $\lambda$  values from grouped model selection, via IC or CV rules, based on multinomial deviance. In the left plot, the two horizontal lines mark average multinomial OOS deviance for independent IC selection of distinct  $\lambda$  values for each response category (based on the Poisson deviances). All selection criteria return values with average OOS deviance within one standard error of the minimum average value. For each IC, the independent Poisson selections are more heavily penalized than their group-learned multinomial-based counterparts. As we will see again in later examples, independent Poisson-based AIC selection is the top performer.

## 5.2 Light beer

Our second example is from the Nielsen Consumer Panel data, available for academic research through the Kilts Center at Chicago Booth ([research.chicagobooth.edu/nielsen](http://research.chicagobooth.edu/nielsen)). This survey tracks purchases by tens of thousands of US households since 2004. We will focus on  $n = 73,128$  purchases of light beer in a number of US markets. The response of interest is brand choice, of a possible five major light beer labels: Budweiser, Miller, Coors, Natural, and Busch. Each purchase is associated with a household that is codified through 16 standard demographic categorical variables: maximum age, total income, main occupation, etc. We've expanded these covariates to 95 binary dummy variables, and included a further 3000 bivariate dummy interactions that are not identically zero, for a total of  $p = 3095$  covariates.

As in the forensic glass example, this is polychotomous regression with  $m_i = 1$  and  $\hat{\mu}_i = 0$  for all observations. Despite this, DMR again does as well as logistic multinomial regression in OOS prediction. Figure 3 plots performance; both DMR and `glmnet` use lasso regularization. Average OOS multinomial deviance  $R^2$  is around 45% for both `glmnet` and DMR under all selection rules *except* the Poisson deviance BIC. We've repeatedly observed such poor performance for this rule. Since the Poisson IC rules tend to favor simpler models than the multinomial IC rules, the BIC's tendency to under-fit is especially harmful. For this reason we use the AIC exclusively in any applications using independent Poisson selection (in particular, whenever joint multinomial IC is computationally infeasible). There is no empirical evidence of advantage for either multinomial IC over the Poisson AIC.

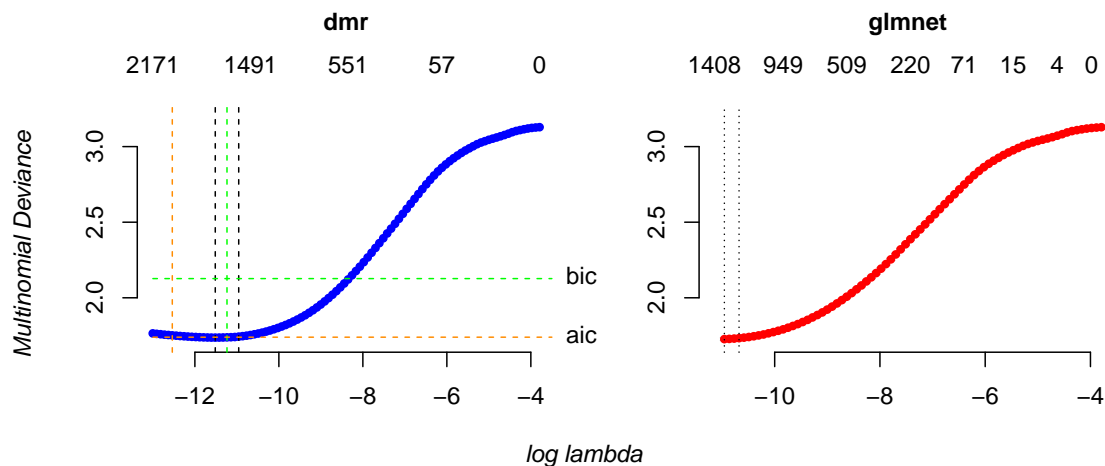


Figure 3: *Light Beer*. OOS deviance for `dmr` and `glmnet` in 20 fold CV, following the same scheme as in Figure 2. The `glmnet` path terminated early (i.e., before  $\lambda_t = \lambda_1/10^4$ ) due to numerical issues.

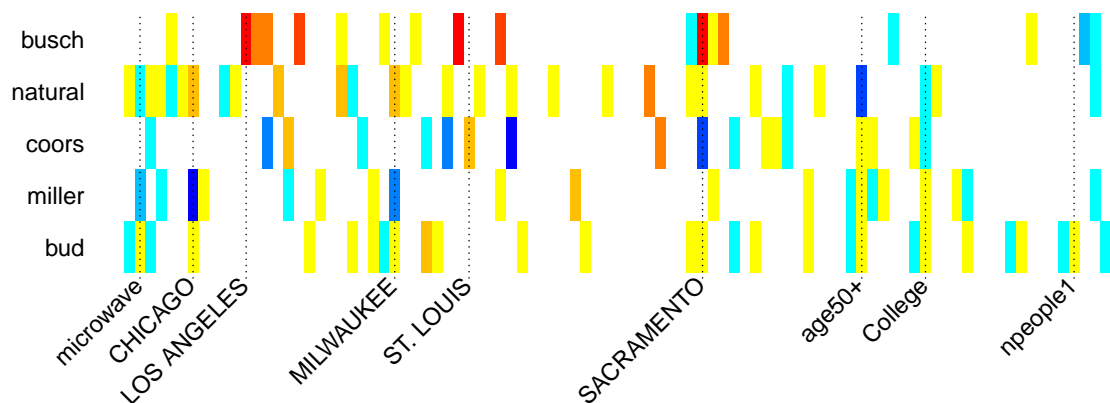


Figure 4: *Light Beer*. Coefficients on the 95 binary main effect variables. The colors show negative  $\hat{\varphi}$  values moving from yellow to red at -4, and positive values moving from light to dark blue at 1. A subset of variable identities are marked along the bottom axis.

Main effect coefficient estimates, using Poisson AIC selection, are illustrated in Figure 4; they are 75% sparse. There are some obvious large effects by market: odds of Busch drop massively (around  $e^4 \approx 55$  lower than baseline) in Los Angeles or Sacramento (Busch is not widely sold in California) while Miller’s odds in Chicago are around 3 times higher than baseline. More subtly, we see that, for example, Miller’s share rises and Bud’s drops in households with a microwave. The set of  $5 \times 3000$  coefficients on dummy interactions is less sparse than the main effects, with only 57% zeros. This includes many large interaction effects that codify unobserved or very rare events, such as the purchase of Natural light by a household in Little Rock AR with oldest member age 30-39 ( $\hat{\varphi} = -7.3$ ).

## 6 MNIR

The previous section shows DMR as a tool for  $D \times$  speedups in polychotomous regression. However, the procedure is really motivated by multinomial applications with large  $D$ . Our main application is multinomial inverse regression (MNIR Taddy, 2013c), a framework for building supervised reduced dimension representations of high dimensional count data. This section outlines MNIR, which will be applied with DMR in our Yelp case study of Section 8.

Inverse regression (IR) is a general strategy for dimension reduction when trying to predict  $K$  dimensional attributes  $\mathbf{v}_i$  from high dimensional (say, of length  $D \gg K$ ) covariates  $\mathbf{x}_i$ . IR is a three stage procedure: first, fit an *inverse model* for  $\mathbf{x}_i | \mathbf{v}_i$ ; second, use the inverse model to obtain *sufficient reduction* (SR) scores  $\mathbf{z}_i$  as reduced dimension projections from  $\mathbf{x}_i$ ; third, fit a low dimensional *forward regression model* for  $\mathbf{v}_i | \mathbf{z}_i$ . In this process the inverse distribution takes the form  $\mathbf{x}_i \sim f(\Phi \mathbf{v}_i)$ , where  $f$  is some parametric (typically natural exponential family) distribution that depends upon  $\mathbf{v}_i$  through the linear operator  $\Phi$ , a  $D \times K$  matrix of loadings. The SR projection is then the  $K$ -vector  $\mathbf{z}_i = \mathbf{x}_i' \Phi$ . Under certain conditions, it holds that  $\mathbf{x}_i \perp\!\!\!\perp \mathbf{v}_i | \mathbf{z}_i$ . Thus all information in  $\mathbf{x}_i$  relevant to  $\mathbf{v}_i$  is summarized in  $\mathbf{z}_i$ , and to predict  $\mathbf{v}_i$  we need model only the  $K$ -variate regression of  $\mathbf{v}_i$  on  $\mathbf{z}_i$ . See Cook (2007) for an overview.

The reason one would want to use IR is its efficiency. Say  $D$ , the dimension of  $\mathbf{x}_i$ , is big relative to  $n$  and that estimation of the parameters in  $\mathbf{v}_i | \mathbf{x}_i$  has a high sampling variance. Assuming an inverse model  $f(\mathbf{x}_i | \mathbf{v}_i)$  introduces information into the estimation problem (a less generous term is ‘bias’) by restricting the relationship between  $\mathbf{x}_i$  and  $\mathbf{v}_i$  to the possibilities parameterized by  $f$ . If  $f$  is close enough to the truth then this restriction will be useful. Cook’s paper includes rigorous efficiency results. We’ve found it helpful to make analogy to the simple arguments used in the related setting of generative classifiers (e.g., as in Efron, 1975, for Gaussian discrimination): you assume higher asymptotic error rates (since  $\mathbf{x}_i$  is a higher dimensional random variable to be modeling than  $\mathbf{v}_i$ ) in exchange for getting near to the optimal rate faster (e.g., through conditional independence assumptions in the inverse/generative distribution).

Taddy (2013c) introduced multinomial inverse regression as a version of IR for dealing with  $\mathbf{x}_i = \mathbf{c}_i$ , covariates that can be characterized as high-dimensional count data. Our primary application is in text mining, where  $\mathbf{c}_i$  is a vector of word (or token, phrase, etc) counts and  $D = \text{length}(\mathbf{c}_i)$  is the size of the vocabulary. The model is just logistic regression, with

$\eta_{ij} = \alpha_j + \mathbf{v}_i' \boldsymbol{\varphi}_j$  the linear model parametrization for the  $j^{th}$  response category (e.g., word) from the  $i^{th}$  observation (e.g., document). Given  $\hat{\boldsymbol{\Phi}} = [\hat{\boldsymbol{\varphi}}_1 \cdots \hat{\boldsymbol{\varphi}}_D]'$  estimated for this logistic regression, MNIR sufficient reduction scores are  $\mathbf{z}_i = \mathbf{c}_i' \hat{\boldsymbol{\Phi}} / m_i$  and we have that  $\mathbf{v}_i \perp\!\!\!\perp \mathbf{c}_i \mid \mathbf{z}_i, m_i$ . The  $1/m_i$  multiplier on here moves projection from word counts to proportions, as in Taddy (2013c), and sufficiency for  $\mathbf{z}_i$  is dependent upon  $m_i$  because we've conditioned on these totals in the multinomial model. The algorithm is completed with forward prediction for  $\mathbf{v}_i$  given  $[\mathbf{z}_i, m_i]$ ; Section 8 uses both simple linear regression and a random forest algorithm.

Analysis, examples, applications of the MNIR framework are in Taddy (2013b,c,d). There are a number of benefits of the approach. First, the IR efficiency argument is especially simple: assuming a multinomial distribution implies that each of the  $M = \sum_i m_i$  count elements are independent observations, such that the sample size for learning  $\boldsymbol{\Phi}$  is now  $M$  rather than  $n$ . That is, in text mining, estimation variance decreases with the number of words rather than the number of documents. Moreover, as we see below via our use of random forests, working with the lower dimensional  $\mathbf{z}_i$  scores allows us to apply powerful nonlinear and ensemble learners that would be infeasible (and unstable) on the full dimensional  $\mathbf{x}_i$ .

Another advantage of MNIR is business oriented: it is a practical way to organize information. In Big data environments, the  $\mathbf{v}_i$  typically contain subsets of attributes that will variously be treated as known or unknown (i.e., conditioned upon or predicted) in future analyses. For example, at a marketing firm  $\mathbf{c}_i$  could be counts for website visits by a specific computer, while  $\mathbf{v}_i$  contains geographic and demographic information along with any observed purchasing behavior. Given a fitted MNIR, the massive set of  $\mathbf{c}_i$  counts can be made available in compact  $\mathbf{z}_i$  scores after mapping through  $\boldsymbol{\Phi}$ . For the analyst to include text data in any modeling related to  $\mathbf{v}_i$  they then need only grab the relevant dimensions of  $\mathbf{z}_i$ . We'll see this tactic in practice in Section 8: text projections on review popularity used first in prediction, and then augmented with projections onto user characteristics for an inference problem.

The final advantage of MNIR has been computational. Taddy (2013c,b) work with very small attribute sets, where  $K < 10$  and often  $K = 1$ . Since sums of multinomials with equal probabilities are also multinomial, one can then *collapse* the modeled counts across equal level-sets of the covariates without affecting the likelihood (continuous covariates can be binned to facilitate collapsing). For example, if  $v_i$  is a univariate binary attribute (e.g., whether

a speaker is Republican in the original MNIR paper) then the logistic multinomial regression has only two observations: the combined counts corresponding to each of  $\{i : v_i = 0\}$  and  $\{i : v_i = 1\}$ . Since collapsing can occur independently for each dimensions of  $\mathbf{c}_i$ , MNIR even works in settings where the original  $n \times D$  count data is too big to store on a single machine.

However, there are many settings with attributes of larger dimension, say  $K$  on the order of hundreds or thousands, where such collapsing is impossible. In Section 8 we have over 400 variables of meta-data associated with each restaurant review. Moreover, the MNIR model is not very believable if  $K$  is small – it seems implausible that only a few factors of interest explain the heterogeneity between individual document word counts. The arguments in Taddy (2013c,d) explain how MNIR can work even if the inverse model is misspecified on an individual level (but is a good fit to the collapsed data). However, there are many settings where this will not hold, and the argument does not apply if you want to interpret individual parameters. In such applications one needs to include a big- $K$  set of explanatory attributes, possibly including many fixed or latent effects. This requires a new computational framework, and it has driven development of DMR. The distribution allows MNIR to work on a previously impossible scale.

## 7 A MapReduce algorithm

We now outline a MapReduce algorithm for analysis of unstructured data via distributed MNIR. MapReduce (MR; Dean and Ghemawat, 2004) is a recipe for analysis of massive datasets, designed to work when the data itself is distributed: stored in many files on a network of distinct machines. The most common platform for MR is Hadoop paired with a distributed file-system (DFS) optimized for such operations (e.g., Hadoop DFS or Amazon’s S3 storage).

A MapReduce routine has three main steps: map, sort, and reduce. The sort is handled by Hadoop, such that the statistician need worry only about map and reduce. The map operation parses unstructured data into a special format. For us, in a text mining example, the mapper program will take a document as input, parse the text into tokens (e.g. words), and output lines of processed token counts: ‘token document | count’. The pre-tab item (our token) is called a ‘key’. Hadoop’s sort facility uses these keys to send the output of your mappers to machines for the next step, reducers, ensuring that all instances of the same key (e.g., the same

word) are grouped together at a single reducer. The reducer then executes some operation that is independent-by-key, and the output is written to file (usually one file per reducer).

Distributed MNIR fits nicely in the MR framework. Our map step tokenizes your unstructured data and organizes the output by token keys. Reduce then takes all observations on a single token and runs a Poisson log regression, applying the gamma lasso with IC selection to obtain coefficient estimates. These are used to build our SR scores, which can be employed in forward regression after the MR routine is done. This recipe is detailed in Algorithm 1.

---

**Algorithm 1** Distributed MNIR

---

**Map:** For each document, tokenize and count sums for each token. Save the total counts  $m_i$  along with attribute information  $\mathbf{v}_i$ . Output `token document | count`.

Combine totals  $m_i$  and attributes  $\mathbf{v}_i$  into a single table, say  $\mathbf{VM}$ . This info can be generated during map or extracted in earlier steps. Cache  $\mathbf{VM}$  so it is available to your reducers.

**Reduce:** For each token key ‘ $j$ ’, obtain a regularization path for Poisson regression of counts  $c_{ij}$  on attributes  $\mathbf{v}_i$  with  $\hat{\mu}_i = \log m_i$ . Apply AIC to select a segment of coefficients from this path, say  $\hat{\varphi}_j$ , and output nonzero elements in sparse triplet format: `word | document | count`.

Each reducer maintains a running total for SR projection,  $\mathbf{z}_i \pm \mathbf{x}'_i \hat{\varphi}_j / m_i$ , output as say  $Z.r$  for the  $r^{th}$  reducer. When all machines are done we aggregate  $Z.r$  to get the complete projections.

The final output is the  $n \times K$  table  $Z$  (or with  $< K$  columns if you don’t need all projection dimensions). The framework is completed in forward regression with  $Z$  and  $\mathbf{VM}$ .

---

We’ve written this as a single MR algorithm, but other variations may work better for your computing architecture. Our most common implementation uses streaming Hadoop on Amazon Web Services (AWS) to execute the map on a large number of files in AWS S3 cloud storage, but replaces the regression reduce step with a simple write, to solid state storage ‘midway’ at the University of Chicago’s Research Computing Center, of token counts tabulated by observation. For example, given 64 reducer machines on AWS the result is 64 text tables on midway, with lines ‘`word | doc | count`’, each containing *all* nonzero counts for a subset of the vocabulary of tokens. These files are small enough to fit in working memory<sup>1</sup> and can be analyzed on distinct compute nodes, each employing another layer of parallelization in looping through Poisson regression for each token. This scheme is able to take advantage of Hadoop

---

<sup>1</sup>If not, use more reducers or split the files.

for fast tokenization of distributed data, and of high performance computing architecture (much faster than, say, a virtual AWS instance) for distributed regression analyses. This is a model that should work well for the many statisticians who have access to computing grids that are designed for high throughput tasks more traditionally associated with physics or chemistry.

## 8 Yelp review popularity prediction

These data were supplied by the review site Yelp for a data mining contest on `kaggle.com`. Full details are at `www.kaggle.com/c/yelp-recruiting/data`; we'll consider the business, user, and review datasets. The reviews, of all sorts of businesses, were recorded on January 19, 2013 for a sample of locations in the southwest US (mostly around Phoenix AZ). The goal of the competition was to predict the combined number of 'funny', 'useful', or 'cool' (f/u/c) votes that a given review receives from other users. Such information can be used by yelp to promote f/u/c reviews before waiting for the users to grade them as such. The example is typical of the problems we encounter in data mining, while it has the advantage that it is publicly available and not so large that we cannot – for comparison – also analyze and cross validate in-memory using a standard lasso.

After removing reviews by unknown users, the data are  $n = 215,879$  reviews on 11,537 businesses by 43,873 users. Business-specific covariates include review- count, star-average, and location, which we model through 61 city fixed effects on top of state effects. Yelp also records a non-exclusive taxonomy of business types; we track membership information for each of the 333 categories containing more than 5 businesses. User covariates are limited to information about past reviews on Yelp: the user's total review count (`usr.count`), their average number of stars given (`usr.stars`), and their previously accumulated count of f/u/c votes (`usr.funny`, `usr.useful`, `usr.cool`; for each observation we subtract that review's f/u/c votes from these totals). Review text was tokenized into words (including combinations of punctuation: potential emoticons) separated by whitespace. After stripping some common suffixes (e.g., 's', 'ing', 'ly') and removing a small set of stopwords (e.g., 'the', 'and', 'or'), we counted frequencies for  $D = 13,938$  words occurring in more than 20 ( $< 0.01\%$ ) of the reviews (total word count is  $M = 17,581,214$ ). In addition to the text, review data includes the star rat-

ing and time ( $t$  and  $t^2$ ) measured in days since posting. Code for tokenization and data processing (and for all the estimation in this section) is available at [github.com/mataddy/yelp](https://github.com/mataddy/yelp).

This yields the following components for our analysis: an  $n \times D$  review-word frequency matrix  $\mathbf{C}$  and  $n$ -vector of row-totals  $\mathbf{m}$ ; the  $n \times 408$  matrix  $\mathbf{U}$  of business, user, and non-text review covariates; and the  $n \times 9$  matrix  $\mathbf{V}$  containing each f/u/c vote count by type and its interaction with the time variables,  $[t, t^2]$ . Columns of both  $\mathbf{U}$  and  $\mathbf{V}$  are scaled to have a standard deviation of one. The multinomial inverse regression model is then

$$\mathbf{c}_i \sim \text{MN}(\mathbf{q}_i, m_i), \quad q_{ij} = e^{\eta_{ij}} / \sum_l e^{\eta_{il}}, \quad \text{where } \eta_{ij} = \alpha_j + \boldsymbol{\varphi}_j^u \mathbf{u}_i + \boldsymbol{\varphi}_j^v \mathbf{v}_i. \quad (6)$$

Each distributed Poisson likelihood that we fit, using  $\hat{\mu}_i = \log m_i$  has the form,

$$c_{ij} \sim \text{Po}(m_i e^{\eta_{ij}}) = \text{Po}(m_i \exp[\alpha_j + \boldsymbol{\varphi}_j^u \mathbf{u}_i + \boldsymbol{\varphi}_j^v \mathbf{v}_i]) \quad (7)$$

with corresponding negative log likelihood proportional to

$$l_j = \sum_i m_i e^{\eta_{ij}} - c_{ij} \eta_{ij} = \sum_i m_i \exp[\alpha_j + \boldsymbol{\varphi}_j^u \mathbf{u}_i + \boldsymbol{\varphi}_j^v \mathbf{v}_i] - c_{ij} (\alpha_j + \boldsymbol{\varphi}_j^u \mathbf{u}_i + \boldsymbol{\varphi}_j^v \mathbf{v}_i). \quad (8)$$

Gamma lasso regularization paths of 20  $\lambda_t$  values are fit for each independent Poisson regression. We use  $\gamma = 1$  in the GL algorithm to achieve concave penalization via path adaptation. Point estimates  $\hat{\boldsymbol{\varphi}}_j$  are selected using AIC based on independent Poisson deviances. We do not consider grouped multinomial-based selection here because of its computational expense.

Regularization paths for a few of the Poisson models are shown in Figure 5. We see, for example, that at our AIC selection the effect of a 1sd increase in review stars multiplies the expected count (or odds, in the multinomial model) for token `: -)` by around  $\exp 0.35 = 1.4$  and for token `: - (` by around  $\exp -0.4 = 0.7$ . In the estimates of our regression model for counts of token `sex`, we see that the word is positively associated with funny votes but negatively associated with useful votes (1sd extra `funny` increases `sex` by around 60%, but 1sd extra `useful` corresponds to a 30% drop in expected `sex`).

Turning to forward regression, denote combined f/u/c votes – the response of interest – by the  $n$ -vector  $\mathbf{y}$ . We consider prediction of  $\log(y_i + 1)$  using covariates  $\mathbf{u}_i$ , review length  $m_i$ ,

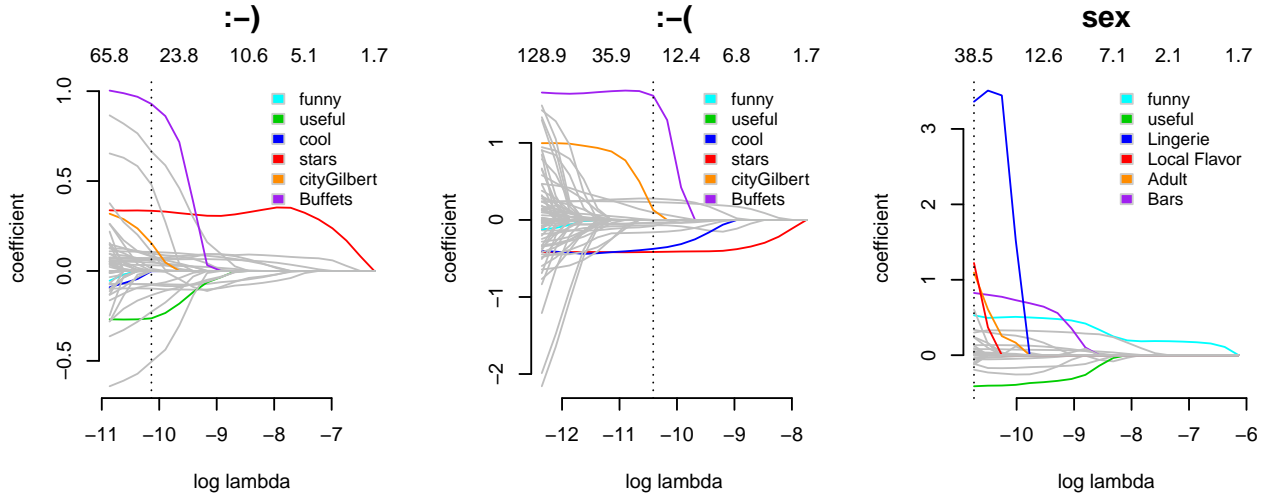


Figure 5: *Yelp*. Inverse regression coefficient regularization paths for counts of the tokens `:-)`, `:-(`, and `sex` regressed onto covariates  $[\mathbf{u}, \mathbf{v}]$ . The legend highlights select covariates, Poisson model degrees of freedom are on the top axis, and our AIC selected estimates are marked with vertical dashed lines.

and the SR projections  $\mathbf{z}_i^v = (1/m_i)\mathbf{c}_i^v\Phi^v$ , with  $\Phi^v = [\varphi_1^v \cdots \varphi_9^v]'$  coefficients for the nine  $f/u/c \times [1, t, t^2]$  variables in  $\mathbf{v}_i$ . Note that we use text SR factors only for variables derived from  $y_i$ ; projection onto  $\mathbf{u}_i$  is ignored unless, as in Section 9, we want to reduce bias in estimation of coefficients on  $\mathbf{u}_i$ . Two algorithms are applied for predicting  $\log(1 + y)$  from  $[\mathbf{U}, \mathbf{Z}^v, \mathbf{m}]$ : ordinary least-squares (OLS), and a 1024 tree random forest (RF; Breiman, 2001) as implemented in the `randomForest` package for R. Results from a 20-fold CV (with each fold left-out for both IR and forward regression) are shown in Figure 6. For comparison, we also show results of straightforward lasso linear regression onto the  $13,938 + 1 + 408 = 14,347$  column input matrix  $[\mathbf{C}/\mathbf{m}, \mathbf{m}, \mathbf{V}]$ , where rows of  $\mathbf{C}/\mathbf{m}$  are word proportions  $\mathbf{c}_i/m_i$ .

Figure 6 shows that average performance of the IR-linear algorithm (MNIR + OLS), using AIC model selection for IR coefficients, is no better than the best straightforward lasso specification (although MNIR is being put to a tougher test here: selecting penalization *within* the CV experiment instead of finding the fixed penalty that performs best across folds). Such performance is typical of what we’ve observed in Big data application.<sup>2</sup> The advantage of

<sup>2</sup>In the comparisons of Taddy (2013c), the IR linear model consistently outperforms a linear lasso comparator in OOS prediction and in compute time. However, the datasets used in that paper are both very small, with  $M \gg n$ . Thus the simple argument in the rejoinder Taddy (2013d) Proposition 1.1 – that, for multinomial IR, estimation variance decreases with  $M$  instead of  $n$  – is working heavily in favor of IR. Examples like the yelp application here are more typical in Big data: even though  $M > n$ , the vocabulary size  $D$  is smaller than  $n$  and straightforward linear regression is already plenty efficient.

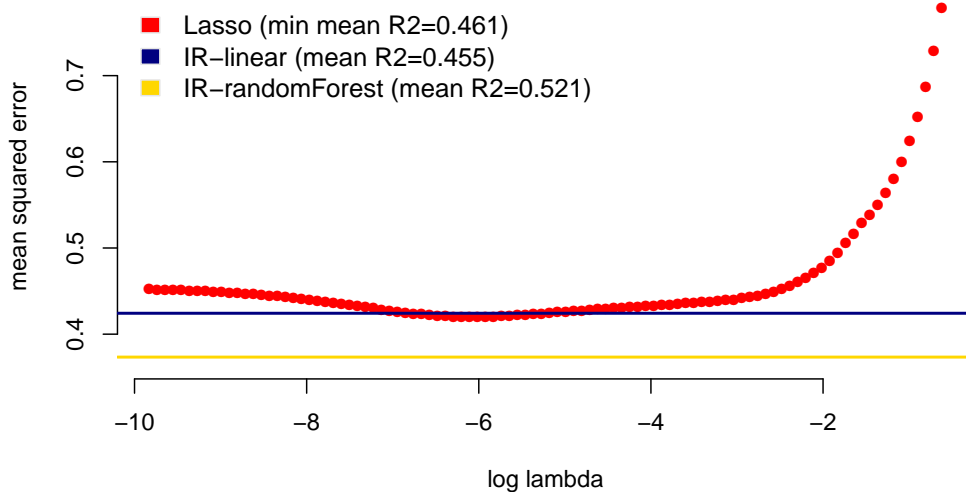


Figure 6: *Yelp*. 20-fold OOS prediction of  $\log(y_i + 1)$ , where  $y_i$  is a reviews combined f/u/c votes. For both inverse regression (IR) procedures, penalization was selected inside the experiment via independent Poisson AIC. The lines and points mark mean OOS MSE, and standard errors are too narrow to see.

MNIR with linear forward regression is then computational: it works in complete distribution and is thus massively scalable (we see in Section 9 that the multinomial model is also useful for structural inference). However the random forest results show another advantage of MNIR: one can deploy flexible nonlinear machine learning on the low dimensional space resulting from SR projection. Methods that are too computationally expensive or unstable on the full covariate set are easy and fast to run on the reduced dimension subspace; our experience with tree methods finds much rich interaction structure that can be exploited after MNIR dimension reduction.

## 9 Inference: estimating the user effect

Machine learning feats are nice – e.g., OOS  $R^2$  greater than 50% on the log number of f/u/c votes – but for staff at Yelp it is likely more important to understand the sources of variation. When a new review is written for a specific business, Yelp can only promote (or not promote) it relative to reviews on the same page. The question is not ‘how popular will this review be?’, but rather ‘should we promote this review over others for this business?’ One way to answer looks at the users: are there certain people who write better reviews? This creates an inference problem – we want to estimate the real effect of user characteristics. This section first describes effect estimation under the setup of Section 8, before investigating how inference can

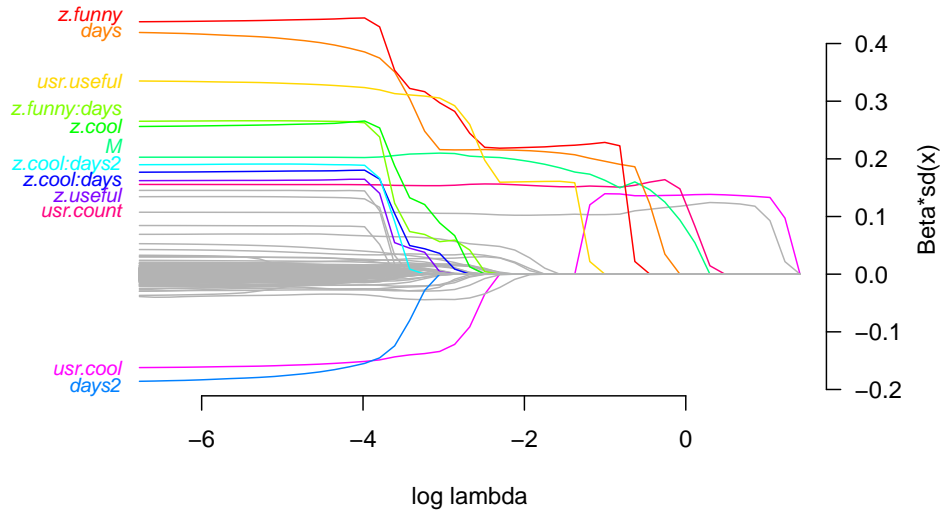


Figure 7: *Yelp*. Forward Poisson log regression of combined f/u/c vote counts onto review attributes  $\mathbf{u}_i$  and text-vote projections  $\mathbf{z}_i^v$ . These are gamma lasso paths with high concavity ( $\gamma = 10$ ).

be improved by conditioning on additional SR projections.

Figure 7 shows regularization paths for Poisson regression (full generalized linear model, not a linear model for  $\log y$ ) of counts  $y_i$  on  $\mathbf{u}_i$  and  $\mathbf{z}_i^v$ . This is a gamma lasso fit with  $\gamma = 10$ , for a very concave penalty (little bias), such that estimates at the end of the path are near the corresponding MLE. As in any multivariate regression, these coefficients represent *partial effects* – change due to individual covariates *after* controlling for the effect of all other inputs. Consider the coefficient on `usr.cool`, a user’s historical count of ‘cool’ votes. This has a negative partial effect (around -0.17 at minimum penalty), despite having a big positive marginal effect (if you follow the path, you’ll see that `usr.cool` is actually the first covariate to enter the model). Thus after you account for the quality predictable by funny or useful votes (particularly useful, which is about twice as common as the others), extra cool votes indicate someone less likely to write popular reviews. This situation occurs because the individual category votes are highly collinear, with correlations between each other of 0.7 to 0.9.

## 9.1 Improved treatment effect estimation

Inference about regression parameters is notoriously difficult in the presence of high dimensional collinear controls. Likelihood maximization for the full 14,347 variable regression in our *Yelp* example, of vote count on all attributes and all text counts, would be very expensive and implies only around 15 observations per covariate. In larger problems,  $n$  and  $\dim(\mathbf{x}_i)$  may

be so large that such a regression is computationally impossible. Unfortunately, the tools that we would usually employ for variable selection (such as a straightforward lasso) will yield biased effect estimates. To see this, consider the regression

$$\mathbb{E}[\log y_i] = \beta_0 + d_i\theta + \mathbf{x}_i'\boldsymbol{\beta} \quad (9)$$

where  $d_i$  is our ‘treatment’ (e.g., user characteristic),  $\theta$  is the effect of interest, and  $\mathbf{x}_i$  is a large vector of control variables (e.g., all other review attributes and the token counts). There will surely be elements of  $\mathbf{x}_i$  that are correlated with  $d_i$ . If we estimate  $\boldsymbol{\beta}$  under lasso penalization, then  $\hat{\beta}_j \neq 0$  only if there is residual effect of  $x_{ij}$  beyond that which can be regressed on  $d_i$ . The effect for these treatment-collinear variables will be conflated into  $\hat{\theta}$ , leading it to be mis-estimated simply because  $d_i$  is correlated with many variables whose effect has been underestimated. The efficiency of the lasso for prediction is now working against us in inference.

In contrast, because the text covariates,  $\mathbf{c}_i$ , enter only through the 9 dimensional SR projection  $\mathbf{z}_i^v$ , we are able to use likelihood maximization to estimate the partial effects of Figure 7. We can improve these estimates still by adding the SR projections  $z_{ik}^u$  corresponding to the treatments of interest. To see why, look again to the treatment effects regression in (9): unbiased estimation of  $\theta$  needs  $\hat{\boldsymbol{\beta}}$  to account both for predictability of  $\log y_i$  from  $\mathbf{x}_i$  and of  $d_i$  from  $\mathbf{x}_i$ . To put it another way, an ideal version of (9) would have  $\mathbb{E}[\log y_i] = \beta_0 + d_i\theta + \beta_y\mathbb{E}[\log y_i|\mathbf{x}_i] + \beta_d\mathbb{E}[d_i|\mathbf{x}_i]$ . Without the  $\beta_d\mathbb{E}[d_i|\mathbf{x}_i]$  term, estimated  $\hat{\theta}$  will be confounded with any effects from  $x_{ij}$  that can be explained by the correlated bit of  $d_i$ . See Belloni et al. (2012) for a much more rigorous and detailed discussion of these issues.

For the same reasons, including in forward regression both  $\mathbf{z}_i^v$  and the relevant elements of  $\mathbf{z}_i^u$ , say  $\mathbf{z}_i^d$  where  $\mathbf{d}_i$  contains the `user.*` elements of  $\mathbf{u}_i$ , more fully controls for the confounding information available in review text. This is straightforward to demonstrate through the MNIR sufficiency results. The model of Figure 7 has  $y_i \perp\!\!\!\perp \mathbf{c}_i | \mathbf{z}_i^v, \mathbf{u}_i, m_i$ , while an augmented *treatment effects MNIR* forward model has  $y_i, \mathbf{d}_i \perp\!\!\!\perp \mathbf{c}_i | \mathbf{z}_i^v, \mathbf{z}_i^d, \mathbf{u}_i \setminus \mathbf{d}_i, m_i$  with  $\mathbf{u}_i \setminus \mathbf{d}_i$  the elements of  $\mathbf{u}_i$  that are considered controls. In the latter procedure, it is the *joint* distribution of  $y_i$  and  $\mathbf{d}_i$  that is made conditionally independent of the text information.

Bootstrap sampling distributions for user characteristic coefficients under this augmented

treatment-effects forward model (regressing  $y_i$  on  $\mathbf{u}_i$ ,  $\mathbf{z}_i^v$ , and  $\mathbf{z}_i^d$ ) are shown in Figure 8.<sup>3</sup> This is a standard sampling-with-replacement nonparametric bootstrap (e.g., Efron, 1994), and both MNIR and forward regression are re-estimated in each bootstrap sample. Figure 8 also includes standard MLE confidence intervals for coefficients on  $\mathbf{d}_i$  in the non-text Poisson regression of  $y_i$  on  $\mathbf{u}_i$ . Comparing the two sets of results, note that the extra variance in the bootstrap sample is due in part to the different distributions being approximated: the confidence intervals condition on observed design  $\mathbf{U}$ , whereas the bootstrap target includes joint covariate-response sampling uncertainty. But we also see that the bootstrap samples are centered away from the confidence intervals for `usr.stars` and `usr.count`. The distinctions are not big here (e.g., for a 1sd increase in `usr.count`, text conditioning moves us from a 19% to a 15% increase in  $\mathbb{E}y_i$ ), but the difference is real and in other contexts could be practically significant.

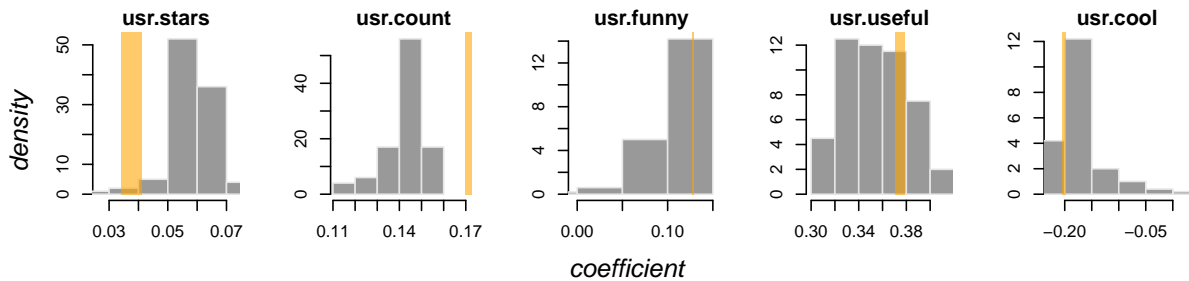


Figure 8: *Yelp*. Inference for user effects. The histograms show 100 bootstrapped coefficient estimates in a model that regresses  $y_i$  on attributes  $\mathbf{u}_i$  and on the MNIR projections for both vote data ( $\mathbf{z}_i^v$ ) and for the user variables of interest (the `usr.*` columns of  $\mathbf{z}_i^u$ ). The orange regions mark 95% confidence intervals ( $\pm 2se$ ) for the corresponding MLE coefficients in regression of  $y_i$  on  $\mathbf{u}_i$  alone.

## 10 Discussion

The distribution of MNIR has opened the opportunity for it to be applied on a new scale, one that is limited only by the number of machines you are able procure. This includes applications where our attribute sets include a large number of fixed or even, in iterative block relaxation algorithms, latent random effects.

<sup>3</sup>To facilitate the repeated model fits required by in bootstrapping, these estimates are actually based on an even faster weighted least-squares approximation instead of the full Poisson inverse regressions. This procedure is detailed in Appendix A, and reduces the time of an MNIR for this *Yelp* data to around 40 seconds on 64 16-core nodes, including data read and result write steps, from the 15 minutes required for an exact Poisson analysis.

This advance is important for our applied work. The collapsing of Taddy (2013c) is useful in pure prediction problems, but today we more often find ourselves addressing inference questions of the type in Section 9. High dimensional attribute sets are essential for such problems because the MNIR model needs to be believable. This is in contrast to pure prediction problems where, as outlined in Taddy (2013d), one can model IR misspecification during forward regression. Moreover, in social science collaboration and in business settings we've found it very valuable to have available a large set of text projections that one can call upon as required.

Finally, the message of this paper has been that Poisson regression (or, via Appendix A, even weighted least squares) enables fast and distributed algorithms for approximating multinomial distributions. It has been pointed out to us that, in unstructured data analysis, a Poisson seems little more arbitrary than a multinomial model. Equation (1) clarifies this issue: the only additional assumption one makes by working with independent Poissons is that the aggregate total,  $m_i$ , is Poisson. We've attempted to mitigate the influence of this assumption, but that is unnecessary if you consider the Poisson a fine model in and of itself.

## References

- Belloni, A., V. Chernozhukov, and C. Hansen (2012). Inference on treatment effects after selection amongst high-dimensional controls. MIT Department of Economics Working Paper No. 12-13.
- Birch, M. W. (1963). Maximum likelihood in three-way contingency tables. *Journal of the Royal Statistical Society - Series B* 25, 220–233.
- Breiman, L. (2001). Random forests. *Machine Learning* 45, 532.
- Cook, R. D. (2007). Fisher lecture: Dimension reduction in regression. *Statistical Science* 22, 126.
- Dean, J. and S. Ghemawat (2004). MapReduce: simplified data processing on large clusters. In *Proceedings of Operating Systems Design and Implementation*, pp. 137150.
- Efron, B. (1975). The efficiency of logistic regression compared to normal discriminant analysis. *Journal of the American Statistical Association* (70), 892898.
- Efron, B. (1994). Missing data, imputation, and the bootstrap (disc p475-479). *Journal of the American Statistical Association* 89, 463475.
- Efron, B. (2004). The estimation of prediction error: Covariance penalties and cross-validation. *Journal of the American Statistical Association* 99, 619–632.
- Gopalan, P., J. M. Hofman, and D. M. Blei (2013). Scalable recommendation with Poisson factorization. arXiv:1311.1704.

- Palmgren, J. (1981). The Fisher information matrix for log linear models arguing conditionally on observed explanatory variable. *Biometrika* 68, 563-566.
- Taddy, M. (2013a). The gamma lasso. arXiv:1308.5623.
- Taddy, M. (2013b). Measuring political sentiment on Twitter: factor-optimal design for multinomial inverse regression. *Technometrics*, to appear.
- Taddy, M. (2013c). Multinomial inverse regression for text analysis. *Journal of the American Statistical Association* 108.
- Taddy, M. (2013d). Rejoinder: Efficiency and structure in MNIR. *Journal of the American Statistical Association* 108, 772-774.
- Tibshirani, R. (1996). Regression shrinkage and selection via the lasso. *Journal of the Royal Statistical Society, Series B* 58, 267-288.
- Venables, W. N. and B. D. Ripley (2002). *Modern Applied Statistics with S* (Fourth ed.). New York: Springer. ISBN 0-387-95457-0.
- Zou, H., T. Hastie, and R. Tibshirani (2007). On the degrees of freedom of the lasso. *The Annals of Statistics* 35, 2173-2192.

## A Weighted least squares approximation

Weighted least squares (WLS) minimization works well with Big data. Because the effect of a coefficient change on the likelihood gradient depends only on the covariances between covariates, one can pre-calculate  $\mathbf{X}'\mathbf{X}$ , where  $\mathbf{X}$  is your matrix of covariates, and never again bother summing over the  $n$  observations. Our use of an IRLS algorithm for estimating Poisson log regressions (Section 3) begs the question: can we fix the weights?

The Poisson regression model for  $c_i$  has intensities  $e^{\eta_i}$ , suppressing response-category subscript  $j$ . Then  $\boldsymbol{\eta} = [\eta_1 \dots \eta_n]$  is our estimation target, with likelihood Hessian matrix  $\mathbf{H} = \text{diag}(e^{\eta_i})$ . Expand a second order Taylor series around the saturated model  $\hat{\eta}_i = \log(c_i)$  (so the gradient disappears) to get the approximate negative log likelihood

$$l(\boldsymbol{\eta}) = (\boldsymbol{\eta} - \log \mathbf{c})' \text{diag}(\mathbf{c})(\boldsymbol{\eta} - \log \mathbf{c}). \quad (10)$$

Writing  $\boldsymbol{\eta}$  out in terms of our fixed-effects regression model yields the approximate Poisson negative log LHD objective  $\sum_i c_i (\alpha + \mathbf{v}_i' \boldsymbol{\varphi} - \log(c_i/m_i))^2$ , a sum of squares with weights  $c_i$

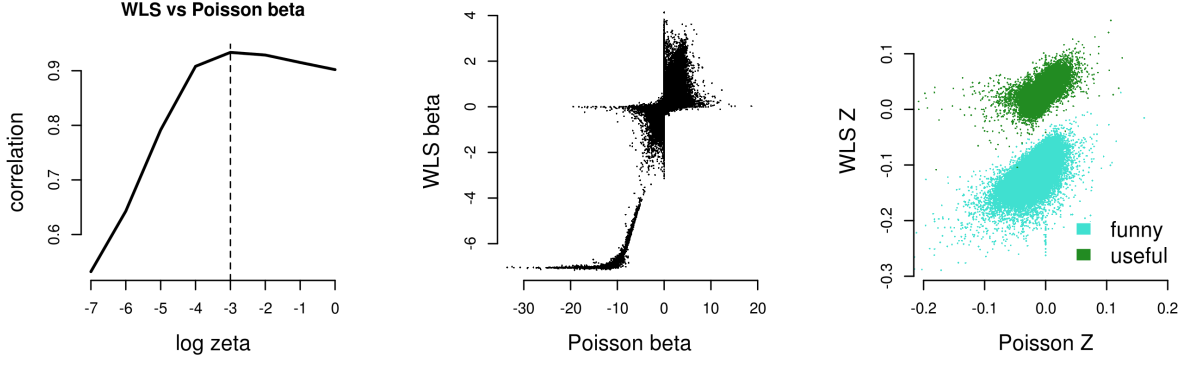


Figure 9: *Yelp*. Weighted least squares approximation. The left plot shows correlation between Poisson coefficient estimates and the WLS values, as a function of buffer  $\zeta$ . At marked  $\zeta = e^{-3} \approx 1/20$ , the center graph plots the estimated values under each method against each other and the right panel shows projection onto two vote categories (useful and cool overlap very closely, so we’ve left cool unplotted).

(=  $c_{ij}$  for each response  $j$ ). This formula will not work in application due to all of the zero values  $c_i$ , but we can add a small buffer term  $\zeta > 0$  to get the *WLS Poisson approximation*

$$l(\alpha, \varphi) = \sum_i \omega_i [\alpha_j + \mathbf{v}_i' \varphi - \log(\omega_i/m_i)]^2, \text{ where } \omega_i = c_i + \zeta. \quad (11)$$

Effect of  $\zeta$  is clearest around  $c_i = 0$ : as the buffer decreases, the weights  $\omega_i$  get smaller while the distance from ‘response’  $\log(\omega_i/m_i)$  to that for  $c_i = 1$ ,  $\log([1 + \zeta]/m_i)$ , gets larger.

The left panel of Figure 9 shows correlation between MNIR  $\hat{\Phi}$  estimates obtained, after AIC model selection, from a Poisson likelihood and from our WLS approximation. The fits are impressively close, especially given that this involves selection after estimation, with a maximum correlation of 0.94 at  $\zeta = 0.05$ . The center panel shows that there are systematic discrepancies: WLS estimates are attenuated, and some big negative  $\hat{\varphi}_{ij}$  estimates from the Poisson fit are thresholded around  $-7$  in WLS. However, the right plot shows that this does not necessarily carry into the implied SR projections. Of primary importance, OOS predictability for MNIR is practically unchanged. Cross validation with  $\zeta = 0.05$  for the *Yelp* example from Section 8, in the same experiment of Figure 6, yields OOS  $R^2$  values of 0.454 for a linear forward model and 0.520 for a random forest – only 0.001 lower than for the exact likelihood.